

First-principle investigation of structural, electronic and magnetic properties of Co_2VIn and CoVIn Heusler compounds

Muthui Zipporah,^{1,2,a,b} Pathak Rohit,^{2,a} Musembi Robinson,^{1,a}
 Mwabora Julius,^{1,a} Skomski Ralph,^{3,a} and Kashyap Arti^{2,a,c}

¹Department of Physics, University of Nairobi, Nairobi 00100, Kenya

²School of Basic Sciences, Indian Institute of Technology, Mandi,
 Himachal Pradesh 175005, India

³Nebraska Center for Materials and Nanoscience and Department of Physics
 and Astronomy, University of Nebraska, Lincoln, Nebraska 68588, USA

(Presented 1 November 2016; received 15 September 2016; accepted 23 October 2016;
 published online 5 January 2017)

Investigation of the structural, electronic and magnetic properties of full-Heusler Co_2VIn as well as half-Heusler CoVIn Cobalt based Heusler compounds using density functional theory (DFT) leads to the general conclusion that Co_2VIn and CoVIn are half-metallic materials with a gap at the Fermi level in the minority states and majority states respectively. A Hubbard-like Coulomb correlation term U has been included in the DFT (DFT+ U) for the computation of the electronic and magnetic properties of the compounds. The structural properties have been calculated for the paramagnetic and ferromagnetic phases, and both Co_2VIn and CoVIn are found to be stable in the ferromagnetic phase. The calculated magnetic moments are $2 \mu_B$ and $0.9 \mu_B$ per formula unit for Co_2VIn and CoVIn respectively. © 2017 Author(s). All article content, except where otherwise noted, is licensed under a Creative Commons Attribution (CC BY) license (<http://creativecommons.org/licenses/by/4.0/>). [<http://dx.doi.org/10.1063/1.4973763>]

I. INTRODUCTION

Heusler compounds consist mainly of full Heusler and half-Heusler families with stoichiometry of X_2YZ and XYZ respectively, where X and Y are transition metal atoms while Z is a main group sp element. Most Co_2YZ Heuslers exhibit half metallic character and half metallic ferromagnetism.¹ They possess desirable properties such as high spin polarizations and magnetic moments as in Co_2FeSi with the highest reported Curie temperature (T_c),¹⁻⁵ structural similarity to industrial binary semiconductors³⁻⁵ and variable localized Co magnetic moments.⁶ Others include a large spin stiffness in interfaces such as $\text{Co}_2\text{MnSi}/\text{MgO}$ as compared to $3d$ metals,⁷ perpendicular magnetic anisotropy (PMA) energy density comparable to Co/Pd,Pt multilayers as in $\text{Co}_2\text{FeAl}/\text{MgO}$ ⁸ and tunable physical properties by alloying with a fourth element as in CoCrFeAl and CoFeAlSi ⁷ among other intriguing features.

Due to their exceptional electronic structure and outstanding properties, they have found application in Magnetic Tunneling Junctions⁹ such as $\text{Co}_2\text{MnSi}/\text{MgO}/\text{Co}_2\text{MnSi}$ with Tunnel Magnetoresistance (TMR) ratios of 1900%,¹⁰ current-perpendicular-to-plane giant magnetoresistance (CPP-GMR) read heads, spin torque oscillators (STO), spin transistors,¹¹ magnetic sensors¹² and non volatile magnetic random access memories.^{13,14} Traditionally, ferromagnetic $3d$ metals have been used in such devices. However, they have a spin polarization of 40% - 50% and they cause problems due to a large difference between their resistance and that of semiconductor substrates.¹⁵⁻¹⁷

^aAll the authors contributed equally to this work.

^bThis research was performed while Muthui Z. was at IIT, Mandi, Himachal Pradesh, 175005, India.

^cElectronic mail: arti@iitmandi.ac.in



The magnetic moments of the Co₂YZ half-metallic ferromagnets follow the localized part of the Slater-Pauling curve. The *sp* element at the Z site plays an important role for the formation of the magnetic moments at the X site¹⁸ and the inclusion of a Hubbard-like Coulomb correlation term *U* in calculations, respects the partial localization of the *d* electrons in the transition metal atoms. The local density approximation (LDA) in density functional theory (DFT) and *U*, (LDA+*U*) was used to reproduce the measured magnetic moment of 6 μ B for Co₂FeSi.¹⁹ It was employed to describe the electronic and magnetic properties of half Heusler CoFeIn and full Heusler Co₂FeIn compounds²⁰ and the experimental magnetic state of Co₂MnSi and Co₂FeSi was well described using *U* values that correspond to those for the Coulomb interaction U_{dd} between *d* electrons in elemental 3*d* transition metals, determined prior to the introduction of the LDA+*U* method.²¹

Heusler compounds Co₂VAl and Co₂VGa have been predicted to be half metallic.²² The next in the series is Co₂VIn. We have investigated the structural, electronic and magnetic properties of full Heusler Co₂VIn and half Heusler CoVIn compounds using DFT and DFT+*U* methods. There are no other experimental or theoretical published results for comparison with the present calculations. Hence, these results can serve as the reference data for further works in this field.

II. COMPUTATIONAL DETAILS

We performed DFT calculations based on the Kohn–Sham formalism of spin-polarized density functional theory using the Vienna Ab Initio Simulation Package (VASP) software. It uses a plane wave basis set and projector-augmented wave (PAW) based pseudo-potentials. Structural optimization has been performed using the generalized gradient approximation (GGA) employing the Perdew-Burke-Ernzerhof (PBE) exchange-correlation functional (PBE-GGA). For the determination of the electronic and magnetic properties, the local spin density approximation L(S)DA, GGA and PBE-GGA as well as DFT+*U* method have been used. Atomic cores were represented by the projector augmented wave method. A Monkhorst–Pack uniform K point grid with 21 x 21 x 21 k points was chosen for geometry optimization and static total energy calculations. Geometries were optimized by relaxing both the unit cell and the positions of all the atoms within the unit cell using the conjugate-gradient algorithm, until a stopping criterion of energy change less than 10⁻⁶ eV was attained. Uniform cut-off energy of 430eV was chosen for all calculations. The integration over the irreducible part of the Brillouin zone was done using the linear tetrahedron method with Blöchl corrections. *U* values of $U_{Co} = 1.92$ eV and $U_V = 1.34$ eV for Cobalt and Vanadium respectively and $J = 0.5$ eV with L(S)DA were applied for the method based on simplified rotationally invariant Dudarev approach implemented in VASP where $U_{eff} = U - J$. *U* values of 0.8eV and $J = 0.5$ eV with PBE-GGA and $U = 1$ eV and $J = 0.5$ eV with GGA resulted in a similar prediction as with L(S)DA + *U*.

III. RESULTS AND DISCUSSION

In this section, we report the structural, electronic and magnetic properties of Co₂VIn and CoVIn, and explain the latter two in terms of the orbital nature of the wave functions near the Fermi level.

A. Geometric properties

The optimized lattice constant for Co₂VIn is 6.001 Å, while that of CoVIn is 5.849 Å as predicted by GGA, while that predicted by LDA is lower as expected at 5.85 Å and 5.7 Å for Co₂VIn and CoVIn respectively. The two Co atoms occupy the 8c ($\frac{1}{4}, \frac{1}{4}, \frac{1}{4}$) position and V and In occupy the ($\frac{1}{2}, \frac{1}{2}, \frac{1}{2}$) and (0, 0, 0) positions respectively in the optimized structure of Co₂VIn while the Co atom occupies the ($\frac{1}{4}, \frac{1}{4}, \frac{1}{4}$) position and V and In occupy the ($\frac{1}{2}, \frac{1}{2}, \frac{1}{2}$) and (0, 0, 0) positions respectively in the optimized structure of CoVIn. On relaxation of unit cell and ionic positions, the cubic structure is maintained. Additionally, the L2₁ structure is found to be more stable than the Hg₂CuTi structure adopted by some Heusler alloys.

The structural properties are calculated in both the paramagnetic and ferromagnetic phases. The total energies optimized in the ferromagnetic phase are lower than the ones in the paramagnetic one, which confirms that the alloys are stable in the ferromagnetic phase. The energy difference between the two phases is 0.876 meV and 0.160 meV for Co₂VIn and CoVIn respectively.

B. Electronic properties

Spin polarized calculations of Co_2VIn and CoVIn Heuslers have been carried out at the equilibrium lattice parameters by employing the L(S)DA, GGA and PBE-GGA approximations. The electronic structure of Co_2VIn obtained from the L(S)DA calculation revealed a gap in the minority states, below the Fermi level resulting in a highly spin polarized band structure at the Fermi level. However, the Fermi level fell within the gap in the minority states when the GGA approximation was employed and the gap widened even further with the PBE-GGA approximation, with the Fermi level moving closer to the center of the gap as shown in Fig. 1.

The electron spin-polarization at the Fermi level is defined by the following expression

$$P = \frac{\rho \uparrow(E_F) - \rho \downarrow(E_F)}{\rho \uparrow(E_F) + \rho \downarrow(E_F)}$$

Where, $\rho \uparrow(E_F)$ and $\rho \downarrow(E_F)$ are the spin dependent densities of states at E_F for the majority and minority-spin cases, respectively. The highest spin polarization is attained from the PBE-GGA calculation. The obtained spin polarizations for all approximations are summarized in Table I.

To obtain a clearer picture of the electronic band structure and to account for electron correlation, we carried out DFT+ U calculations in order to treat the electron-electron correlations on localized d states of Co and V. The $U_{\text{eff}} = U - J$, was used to correct the double counted terms. With L(S)DA approximation, the U values used by Kandpal *et al.*²² in studying the electronic properties of systems such as Co_2VAI which is isoelectronic and isostructural to Co_2VIn , worked excellently predicting 100% spin polarization. In order to reproduce a similar result as with L(S) DA, coulomb correlation values U required for GGA and PBE-GGA were much lower than those with L(S) DA, possibly due to improved estimation of coulomb correlation in these approximations and was determined using the U ramping up method.

The inclusion of U in the calculation causes the band gap in the minority states of Co_2VIn to open up to an average of 0.2 eV as recorded in Table I, with the lowest conduction band at the G point shifting to higher energies. In addition, 100% spin polarization is realized with all approximations

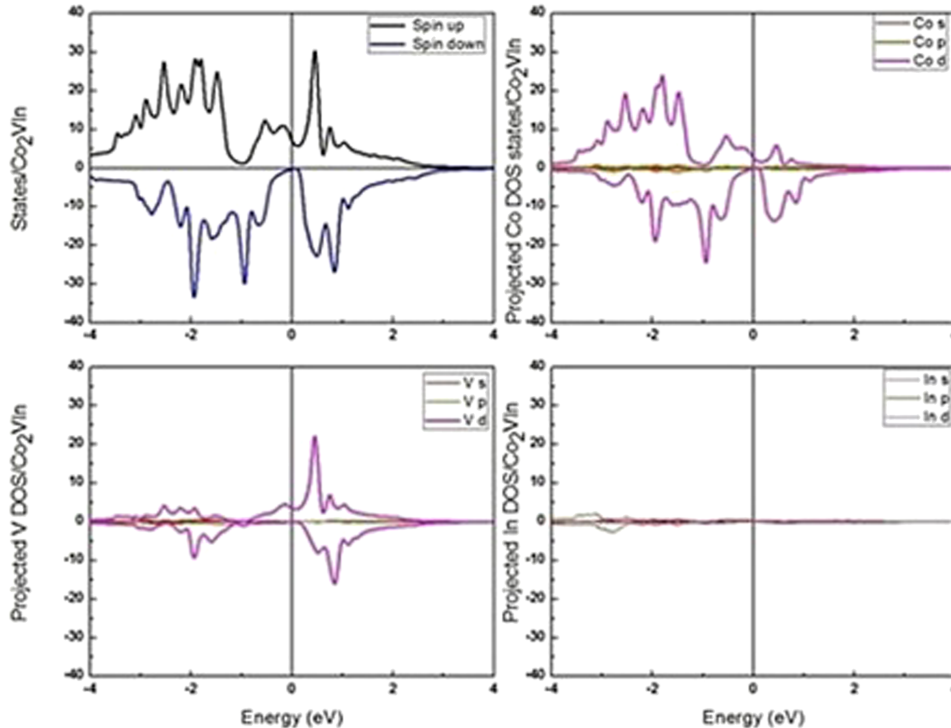


FIG. 1. TDOS and Partial DOS for Co_2VIn for Co, V and In using PBE-GGA approximation.

TABLE I. The calculated results for spin Polarization and Band Gaps for Co_2VIn and CoVIn obtained using L(S)DA, L(S)DA+U, GGA, GGA+U, PBE-GGA and PBE-GGA+U approximations.

	Co_2VIn		CoVIn	
	Spin Polarization	Minority states Band Gap (eV)	Spin Polarization	Majority states Band Gap (eV)
L(S)DA	86.28%	0.00	87.32%	0.20
GGA	98.38%	0.07	88.65%	0.20
PBE-GGA	99.40%	0.09	94.07%	0.27
PBE-GGA+U	100.00%	0.19	100.00%	0.08
L(S)DA+U	100.00%	0.21	100.00 %	0.18
GGA+U	100.00%	0.20	100.00%	0.18

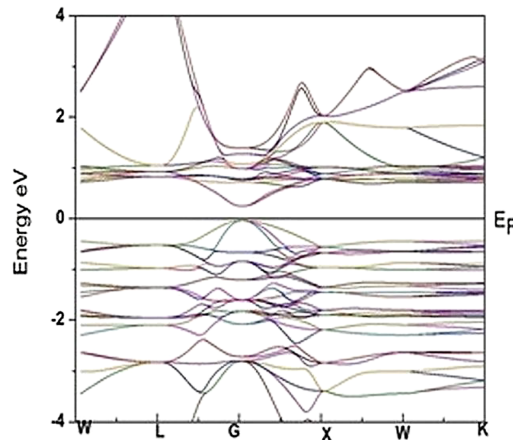
with the Fermi level almost at the centre of the gap. This confirms the half metallic characteristic with the charge transport being dominated by the spin-up electrons. The corresponding spin resolved band structures along the high symmetry directions are consistent with the total density of states plots as depicted by the minority spin band structure plot for Co_2VIn in Fig. 2.

The band gap in Co_2VIn can be explained to be as a result of hybridization between the two Co and V $3d$ orbitals. The e_g and t_{2g} states of the Co and V sites dominate the part of the plots around E_F as shown in Fig. 1 for both spin channels. A closer look at the atomic resolved DOS in Fig. 1 reveals that V atoms present a broad spin down gap unlike Co sites around E_F .

The minority states around the gap therefore are localized at the Co sites and do not couple to V. This therefore means that the gap occurs between antibonding states formed after the hybridization between Co $3d$ orbitals commonly referred to as t_{1u} (d_{xy} , d_{yz} and d_{zx}) represented by the peak below the Fermi level and e_u (d_{z^2} and $d_{x^2-y^2}$) states represented by the peak above the Fermi level, that do not hybridize with V states, as they do not transform with the same representation. This therefore explains why the band gaps are small, which is characteristic of $d-d$ band gaps.

The L(S)DA calculation for CoVIn yielded a highly spin polarized total density of states at the Fermi level, with a gap in the majority states and the Fermi level located closer to the valence band. The spin polarization was not 100% as some majority states were present at the Fermi level. The density of states plots were similar for the three approximations the only difference being the slight shift of the Fermi level towards the center of the gap as the approximations were varied from L(S)DA to PBE-GGA resulting in higher spin polarizations. The total and partial density of states plot for CoVIn are depicted in Fig. 3.

The spin resolved band structures obtained using GGA+U for CoVIn revealed that the minority states are conducting while a band gap exists at the Fermi level for the majority states. The GGA+U

FIG. 2. Spin down electronic band structure of Co_2VIn at the equilibrium lattice parameter using DFT+U approximation.

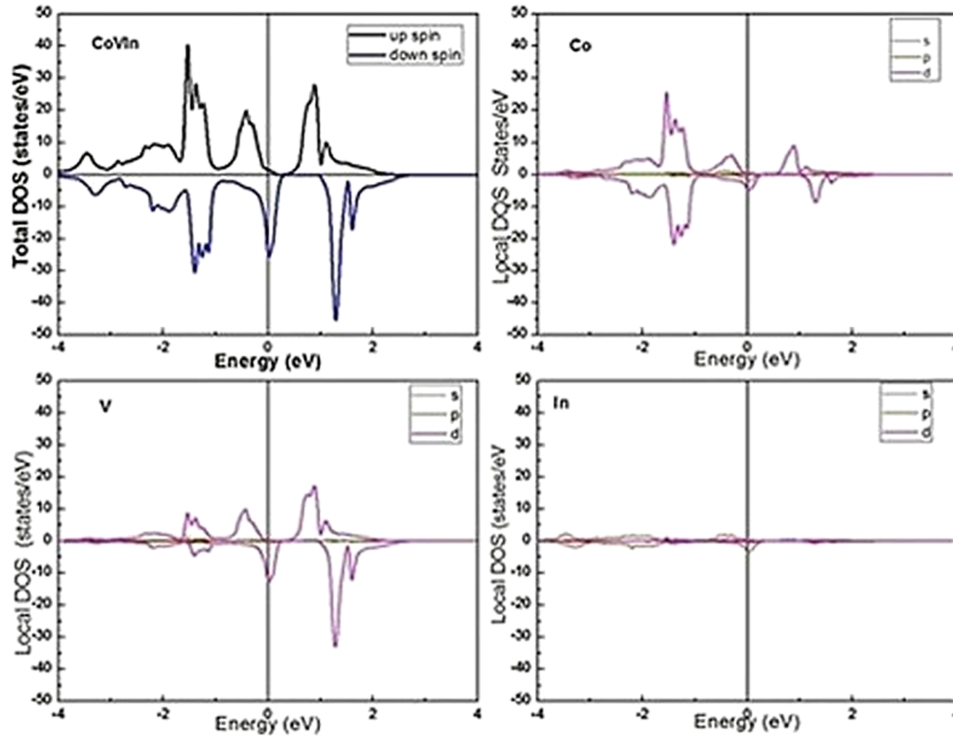


FIG. 3. TDOS and Partial DOS for CoVIn for Co, V and In using PBE-GGA approximation.

scheme resulted in 100% spin polarization of states, with only the minority states at the Fermi level. The partial density of states plots revealed the domination of the 3d electrons of both Co and V around the Fermi level resulting in a hybridization gap with the bonding t_{2g} (d_{xy} , d_{yz} and d_{zx}) states forming the peak just below the E_F and the peak just above E_F resulting from the antibonding e_g (d_z^2 and $d_{x^2-y^2}$) states. This is well depicted in Fig. 3. The spin polarization results as well as band gaps are summarized in Table I.

For both Heusler compounds Co_2VIn and CoVIn , our results show that the majority and the minority spin channels of both Heusler alloys do not display a similar distribution, implying spin polarization. DFT+U emerges as a powerful technique of treating the d states of the transition metals in these type of systems, revealing the expected fully spin polarized electronic structures.

C. Magnetic properties

The Slater Pauling rule predicts the total magnetic moment in Heusler alloys. For the full Heusler alloy it is $M_T = Z_T - 24$ and for the half Heusler alloys it is $M_T = Z_T - 18$, where M_T is the total magnetic moment per unit cell and Z_T is the total number of valence electrons.²³ For Co_2VIn and CoVIn , the magnetic moments predicted by the Slater Pauling rule are 2 μB and 1 μB respectively. This comes about when the number of occupied states is fixed at twelve for Co_2VIn and nine for CoVIn for the minority and majority states respectively due to hybridization resulting in the formation of a half metallic gap typical of Heuslers. In this case, the calculated values are very close to these predicted integer values differing by between 0.024 μB and 0.16 μB as predicted by L(S)DA and PBE-GGA+U respectively but in full agreement with the GGA moments. These are summarized in Table II together with the moments predicted for each site.

The results for the magnetic moments of Co_2VIn in Table II follow the exact trend as those obtained from a study of the magnetic properties of Co_2VAl and Co_2VGa which are isoelectronic and isostructural to Co_2VIn , in which Co and V were found to couple ferromagnetically with magnetic moment values of 0.94 and 0.22 μB for Co and V respectively for Co_2VAl and 0.98 and 0.15 μB for Co and V respectively for Co_2VGa using full potential linearised augmented plane wave method

TABLE II. The calculated results for magnetic moments for Co₂VIn and CoVIn obtained using L(S)DA, L(S)DA+U, GGA, GGA+U, PBE-GGA and PBE-GGA+U approximations.

		Total Magnetic Moment	Co	V	In
L(S)DA	Co ₂ VIn	1.985	0.892	0.235	-0.034
	CoVIn	0.828	0.159	0.596	0.073
L(S)DA+U	Co ₂ VIn	2.016	1.037	0.005	-0.063
	CoVIn	0.892	-0.240	1.065	0.074
GGA	Co ₂ VIn	2.001	0.928	0.192	-0.047
	CoVIn	0.852	0.095	0.684	0.074
GGA+U	Co ₂ VIn	2.031	1.091	-0.074	-0.078
	CoVIn	0.902	-0.532	1.370	0.067
PBE-GGA	Co ₂ VIn	2.011	0.968	0.131	-0.056
	CoVIn	0.879	-0.020	0.829	0.070
PBE-GGA+U	Co ₂ VIn	2.030	1.069	-0.029	-0.078
	CoVIn	0.919	-0.780	1.658	0.041

(FLAPW) within PBE-GGA.¹⁸ This trend is well replicated in our results where a reduction in the V moment is resulting in an increase in the Co moment, with the total moment varying not by more than 0.04 μ B. The total magnetic moment of Co₂VIn is mainly contributed by the Co and V sites, where these contributions are due to the large exchange splitting in the Co and V atoms for the majority-spin and minority-spin channels as depicted by the partial density of states plots in Figure 1.

The In atoms have a negligible local moment with opposite sign in comparison with the Co and V elements. In this regard, In, though larger than Al and Ga yields a similar outcome. Its 5*p* states have an anti-parallel interaction due to *p-d* hybridization to the 3*d* Co and 3*d* V orbitals of the transition elements.

All except GGA and L(S)DA schemes predict a ferrimagnetic coupling between Co and V in CoVIn. In a study of magnetic properties of Co₂FeSi, L(S)DA+*U* was found to yield magnetic moment values in agreement with experiment but not GGA or LDA.¹⁹ In a study of the electronic properties of CoVSb, the moments of Co and V were found to be -0.20 and 1.12 μ B using PBE-GGA.¹⁸

As is evident from Table II, the more electron correlation is put into consideration, the higher the total magnetic moments. In the case of CoVIn, 3*d* V states contribute most of the moment.

IV. CONCLUSION

While Co₂VIn displays conventional half metallic characteristics, CoVIn displays a half metallic gap in the majority states, with neither the application of an external field nor doping. Therefore, these findings highlight two new promising half-metallic materials toward realistic spintronics applications.

ACKNOWLEDGMENTS

Muthui Z. acknowledges the support of OWSD fellowship and IIT, Mandi.

- ¹ T. Graf, C. Felser, and S. S. P. Parkin, "Simple rules for the understanding of Heusler compounds," *Prog. Solid State Chem.* **39**(1), 1–50 (2011).
- ² B. K. Hazra, M. M. Raja, and S. Srinath, "Correlation between structural, magnetic and transport properties of Co₂FeSi thin films," *J. Phys. Appl. Phys.* **49**(6), 65007 (2016).
- ³ I. Galanakis, K. Özdoğan, E. Şaşioğlu, and B. Aktaş, "Ferrimagnetism and antiferro-magnetism in half-metallic Heusler alloys," *Phys. Status Solidi A* **205**(5), 1036–1039 (2008).
- ⁴ L. Feng, E. K. Liu, W. X. Zhang, W. H. Wang, and G. H. Wu, "First-principles investigation of half-metallic ferromagnetism of half-Heusler compounds XYZ," *J. Magn. Magn. Mater.* **351**, 92–97 (2014).
- ⁵ R. Umamaheswari, M. Yogeswari, and G. Kalpana, "Ab-initio investigation of half-metallic ferromagnetism in half-Heusler compounds XYZ (X=Li, Na, K and Rb; Y=Mg, Ca, Sr and Ba; Z=B, Al and Ga)," *J. Magn. Magn. Mater.* **350**, 167–173 (2014).
- ⁶ A. W. Carbonari, R. N. Saxena, W. Pendl, Jr., J. Mestnik Filho, R. N. Attili, M. Olzon-Dionysio, and S. D. de Souza, "Magnetic hyperfine field in the Heusler alloys Co₂YZ (Y = V, Nb, Ta, Cr; Z = Al, Ga)," *J. Magn. Magn. Mater.* **163**(3), 313–321 (1996).

- ⁷ S. Trudel, O. Gaier, J. Hamrle, and B. Hillebrands, "Magnetic anisotropy, exchange and damping in cobalt-based full-Heusler compounds: an experimental review," *J. Phys. Appl. Phys.* **43**(19), 193001 (2010).
- ⁸ W. Wang, H. Sukegawa, and K. Inomata, "Perpendicular magnetic anisotropy of Co₂FeAl/Pt multilayers for spintronic devices," *Appl. Phys. Express* **3**(9), 93002 (2010).
- ⁹ M. A. Tanaka, Y. Ishikawa, Y. Wada, S. Hori, A. Murata, S. Horii, Y. Yamanishi, K. Mibu, K. Kondou, T. Ono, and S. Kasai, "Preparation of Co₂FeSn Heusler alloy films and magnetoresistance of Fe/MgO/Co₂FeSn magnetic tunnel junctions," *J. Appl. Phys.* **111**(5), 53902 (2012).
- ¹⁰ L. Wollmann, S. Chadov, J. Kübler, and C. Felser, "Magnetism in cubic manganese-rich Heusler compounds," *Phys. Rev. B* **90**, 214420 (2014).
- ¹¹ Z. Wen, T. Kubota, T. Yamamoto, and K. Takahashi, "Fully epitaxial C1b-type NiMnSb half-Heusler alloy films for current-perpendicular-to-plane giant magnetoresistance devices with a Ag spacer," *Sci. Rep.* **5**, 18387 (2015).
- ¹² X.-P. Wei, J.-B. Deng, G.-Y. Mao, S.-B. Chu, and X.-R. Hu, "Half-metallic properties for the Ti₂YZ (Y=Fe,Co,Ni,Z=Al,Ga,In) Heusler alloys: A first-principles study," [ArXiv11105411](https://arxiv.org/abs/1110.5411) Cond-Mat, Oct. 2011.
- ¹³ Z. Ren, Y. Liu, S. Li, X. Zhang, and H. Liu, "Site preference and electronic structure of Mn₂RhZ (Z = Al, Ga, In, Si, Ge, Sn, Sb): a theoretical study," *Mater. Sci.-Pol.* **0**(0) (2016).
- ¹⁴ S. N. Holmes and M. Pepper, "Cobalt-based Heusler Alloys for spin-injection devices," *J. Supercond.* **16**(1), 191–194 (2003).
- ¹⁵ P. Klaer, "Disentangling the Mn moments on different sublattices in the half-metallic ferrimagnet Mn₃?xCoxGa," *Appl. Phys. Lett.* (2012).
- ¹⁶ Y. Ma, X. Li, Q. Sun, and B. Huang, "Prediction of two-dimensional materials with half-metallic dirac cones: Ni₂C₁₈H₁₂ and Co₂C₁₈H₁₂," *Elsevier* **73**, 382–388 (2014).
- ¹⁷ J. C. Woo, H. Hasegawa, Y. S. Kwon, T. Yao, and K. H. Yoo, *Compound Semiconductors 2004: Compound Semiconductors for Quantum Science and Nanostructures* (CRC Press, 2005).
- ¹⁸ S. E. Kulkova, S. V. Ereemeev, T. Kakeshita, S. S. Kulkov, and G. E. Rudenski, "The electronic structure and magnetic properties of full- and half-Heusler alloys," *Mater. Trans.* **47**(3), 599–606 (2006).
- ¹⁹ H. C. Kandpal, G. H. Fecher, C. Felser, and G. Schönhense, "Correlation in the transition-metal-based Heusler compounds Co₂MnSi and Co₂FeSi," *Phys. Rev. B* **73**(9), 94422 (2006).
- ²⁰ M. ElAmineMonir, R. Khenata, H. Baltache, G. Murtaza, M. Abu-Jafar, D. Rached, S. BinOmran, and A. Bouhemadou, "Study of structural, electronic and magnetic properties of CoFeIn and Co₂FeIn Heusler alloys," *jmmm, Journal of Magnetism and Magnetic Materials* **394**, 404–409 (2015).
- ²¹ T. Graf, C. Felser, and S. S. P. Parkin, "Heusler compounds: Applications in spintronics," in *Handbook of Spintronics*, edited by Y. Xu, D. D. Awschalom, and J. Nitta (Springer, Netherlands, 2016), pp. 335–364.
- ²² H. C. Kandpal, G. H. Fecher, and C. Felser, "Calculated electronic and magnetic properties of the half-metallic, transition metal based Heusler compounds," *J. Phys. Appl. Phys.* **40**(6), 1507 (2007).
- ²³ S. Krishnaveni, M. Sundaeswari, and M. Rajagopalan, "Prediction of electronic and magnetic properties of full Heusler Alloy–Ir₂CrAl," *IOSR J. Appl. Phys. IOSR-JAP* **7**, 52–55 (2015).